Electronic Supplementary Information

Electro-deoxidation behavior of solid SeO_2 in low-temperature molten salt

Cheng Chang[a], Jiguo Tu[a,c,*], Yunfei Chen[a], Mingyong Wang[a], Shuqiang Jiao[a,b,*]

[a] State Key Laboratory of Advanced Metallurgy, University of Science and Technology Beijing, Beijing 100083, PR China

[b] School of Metallurgical and Ecological Engineering, University of Science and Technology Beijing, Beijing 100083, PR China

[c] Beijing Key Laboratory of Green Recovery and Extraction of Rare and Precious Metals, University of Science and Technology Beijing, Beijing 100083, PR China

***Corresponding Author**

E-mail addresses: jtu15@ustb.edu.cn (Jiguo Tu), sjiao@ustb.edu.cn (Shuqiang Jiao)

Experimental section

Preparation of molten salt electrolyte, pre-electrolysis, electrochemical testing, and constant potential electrolysis/electro-deoxidation were all performed in a glove box filled with Ar (Jinghui, 99.999%). Before each measurement, the electrodes were polished by 10000 mesh sandpaper, washed with alcohol for 10 minutes by ultrasonic and dried at 110 °C.

Preparation of molten salts

The molten salt electrolyte was prepared by mixing NaCl (Aladdin, 99.5%, drying at 200 °C for 10 h) and $AlCl_3$ (Aladdin, AR). The NaCl-$AlCl_3$ (1.1:1 mol) was placed in a sealed glass electrolytic cell with Ar, heated at 463.15 K for 2 h to form a uniform translucent yellow liquid. A small amount of unmelted solid NaCl precipitated in the bottom of the electrolytic cell (Fig. S1a), which keeps the Cl^- ions concentration. At 463.15K, the liquid phase composition of the saturated NaCl molten salt is $AlCl_3$(l):NaCl(l) = 0.496:0.504 mol, which is a Lewis neutral molten salt. Se (Acros, 99.9%) and SeO_2 (Acros, 99.8%) reagents were used as the working electrodes.

Pre-electrolysis of molten salts

The constant potential pre-electrolysis was performed to remove impurities in the molten salt by CHI600E electrochemical workstation (CH Instruments). The CV measurement (Fig. S1b) of blank molten salt was conducted at 463.15 K at a sweep rate of 100 mV s^{-1}, with Pt wire as the quasi-reference electrode, Mo sheet as the counter electrode, and Mo microcavity electrode (BW[§]) as the working electrode (Fig. S2b). CV curves of the molten salt without pre-electrolysis in Fig. S1b indicated that the peak of impurity was appeared before -1.2 V (vs. Pt), thus the pre-electrolysis potential was -1.2 V (vs. Pt). The three-electrode system of pre-electrolysis was adopted with Mo sheet as the counter electrode, a coiled Mo wire as the working electrode, and Pt wire as the quasi-reference electrode (Fig. S2a). After pre-electrolysis, the molten salt appeared light transparent yellow, and the impurities deposited in the glass sleeve of the coiled Mo wire electrode could be observed (Fig.

S1c). Then CV measurement of the molten salt after pre-electrolysis was used to determine whether or not to remove the impurities (sweep rate: 100 mV s^{-1}; quasi-reference electrode: Pt or Al wire; counter electrode: Mo sheet; working electrode: Mo microcavity electrode (BW[§]); Fig. S2b). Since Al was susceptible to corrosion in this molten salt, Pt quasi-reference electrode was used in the following experiments.

Property testing of pre-electrolyzed molten salts

A constant potential electrolysis at -1.5 V (vs. Pt) was conducted for 6 h in the pre-electrolyzed molten salt, with Mo sheet as the counter electrode, Mo sheet as the working electrode, and Pt wire as the quasi-reference electrode (Fig. S2c). The working electrode after electrolysis was analyzed by XRD (Rigaku, D/max-RB) and SEM (JEOL, JSM-6701F). It was used to observe the decomposition products of molten salts. The pre-electrolyzed molten salt (60 g) with the addition of SeO_2 (2 g) were held at 463.15 K for 12 h. And the upper clear layer of molten salt was subjected to ICP detection (Agilent, 7850) to determine the solubility of SeO_2. To further proved that the system can be used as a medium to transport O^{2-} ions, the blank molten salt (60 g) and the molten salt (60 g) with the addition of oxides (2g Na_2O or 2g Al_2O_3) were held at 463.15 K for 12 h. And the compositions of the upper transparent molten salt layers were clearly understood through XPS (Kratos, AXIS Ultra DLD).

Clarify the electro-deoxidation process

The deoxidation process of SeO_2 was investigated by combining the thermodynamic analysis, electrochemical techniques, and phase identification. The SeO_2 electro-deoxidation process was investigated at 463.15 K through a three-electrode configuration, in which Mo sheet was used as the counter electrode, Pt wire was used as a quasi-reference electrode, and Mo microcavity electrode filled with SeO_2 (OW[§§]) or Se (SW[§§§]) as the working electrode (Fig. S2b). CV was measured from 10 to 100 mV s^{-1}, and square wave voltammogram (SWV) was performed from 5 to 50 Hz. The electro-deoxidation of SeO_2 at 463.15 K was performed under different potentials, using Mo sheet as the counter electrode, SeO_2 cylindrical pellet wrapped in Mo mesh

(10 MPa pressing, 15 mm diameter) as the working electrode, and Pt wire as the quasi-reference electrode (Fig. 1d). The Mo sheet after electrolysis was analyzed by XRD and SEM. The upper transparent layer of molten salt after electro-deoxidation at -0.2 V (vs. Pt) for 8 h was clearly understood through XPS. The compositions and morphology changes of SeO_2 electro-deoxidation products under different potentials were clearly understood through XRD, XPS and SEM.

Notes

§ Blank Mo microcavity electrode

§§ Mo microcavity electrode filled with SeO_2

§§§ Mo microcavity electrode filled with Se

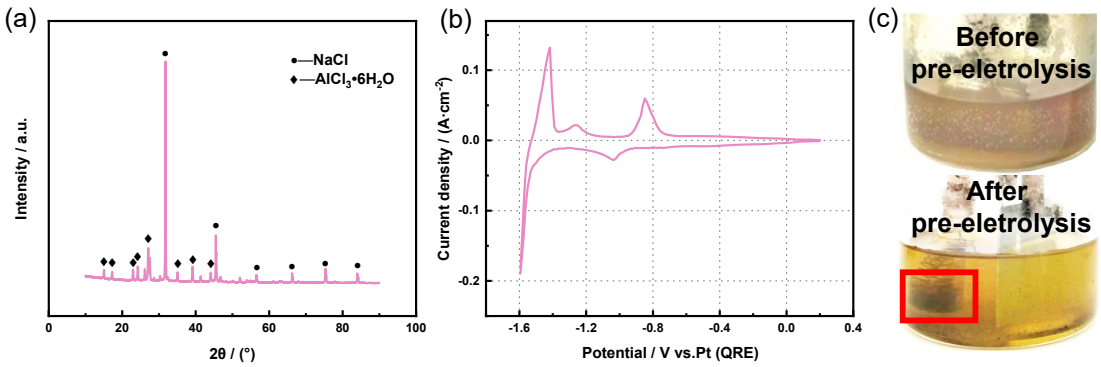

Fig. S1. (a) XRD pattern of the insoluble material at the bottom of molten salt. (b) CV curve of the molten salt before pre-electrolysis at a scan rate of 100 mV s^{-1}. (c) The photos of the molten salt before and after pre-electrolysis (Red frame: impurities deposited in the glass sleeve of the working electrode).

The insoluble NaCl (Fig. S1a) at the bottom of the molten salt ensured the neutralization of molten salt.

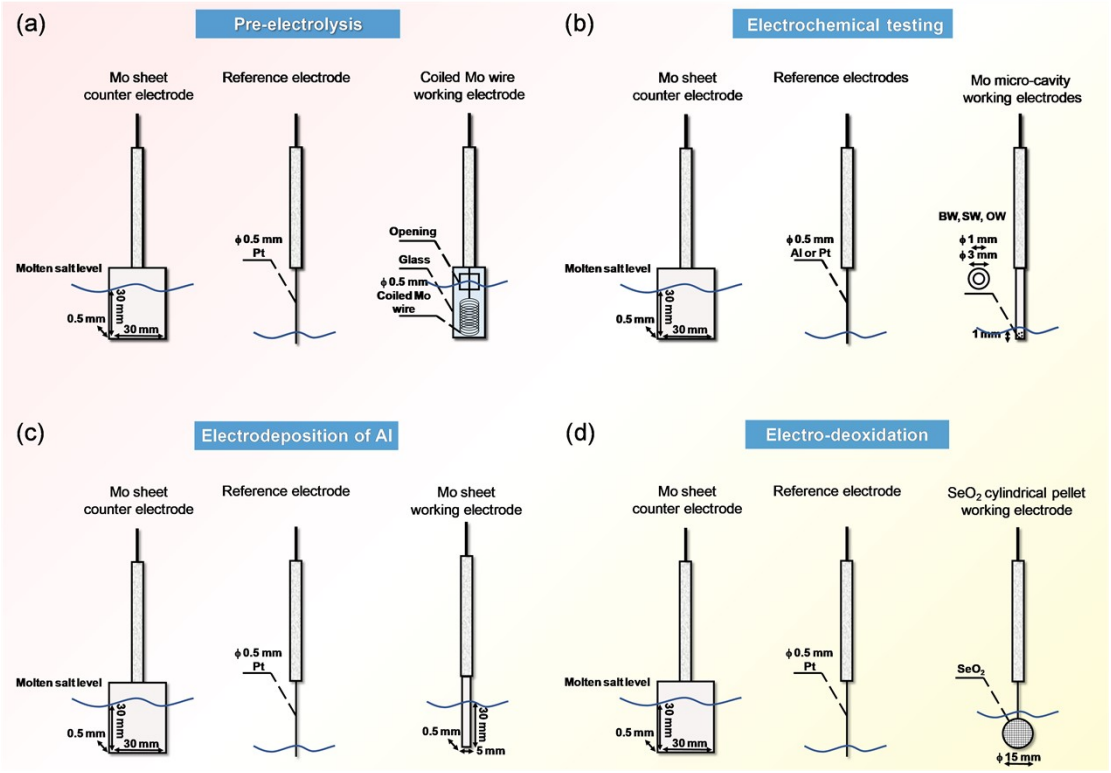

Fig. S2. Schematic diagrams of electrodes for (a) pre-electrolysis, (b) electrochemical testing, (c) electrodeposition of Al, and (d) electro-deoxidation involved in the experiment.

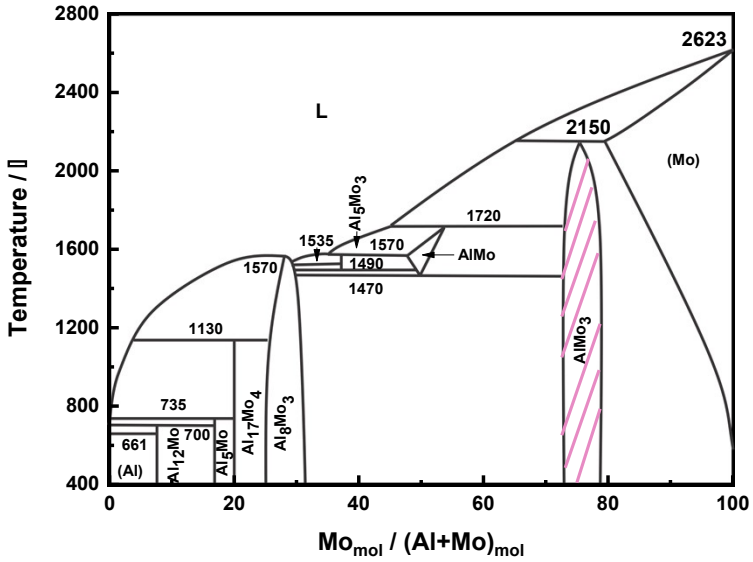

Fig. S3. Al-Mo phase diagram.

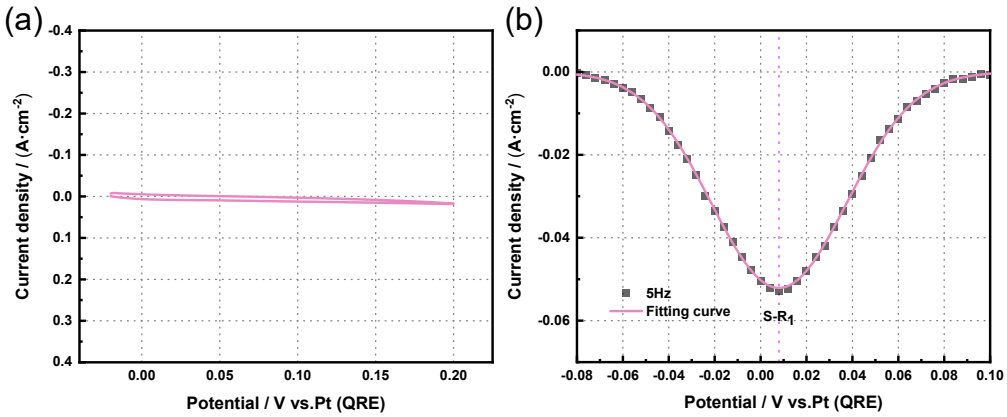

Fig. S4. (a) The first CV curve of OW electrode system scanned from the OCP potential forward to 0.2 V (vs. Pt) at 100 mV s^{-1}. (b) The SWV curve of the SW electrode system at 5 Hz and the fitting curve.

For comparison, the SW system was oxidized at a constant potential of 0.1 V (vs. Pt) for 4 h to ensure the complete oxidation of Se, and then it was performed by SWV at 5Hz (Fig. S4b).

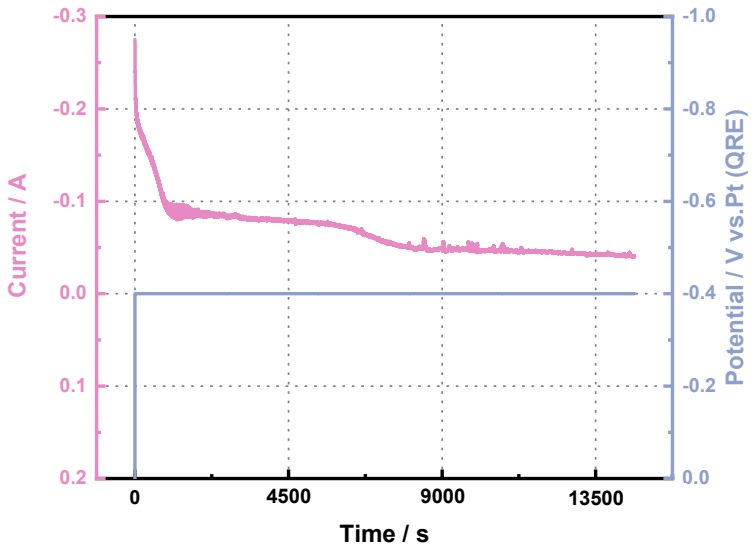

Fig. S5. Current-time curve of SeO_2 at a constant potential of -0.4 V (vs. Pt) for 4 h.

After SeO_2 cylindrical pellet electrodes were deoxidized for 4 h at -0.4 V (vs. Pt), the typical current-time curve was shown in Fig. S5. At the beginning of electrolysis, the large current would be not sustained due to the low concentration of oxide ions, leading to the sharp decrease on current. As the Faraday process proceeds further, the oxide ions generated by electrode-deoxidation transfer to the interior of the molten salt. As the reduction reaction continues, the curve gradually presents the first current shoulder, corresponding to the first step of the two-electron electro-deoxidation process (Se(IV)→Se(II)). After 7000 s, the curve reaches the second current shoulder, corresponding to the second step of the two-electron electro-deoxidation (Se(II)→Se(0)). It was demonstrated that the cathodic process was a two-step, two-electron process.

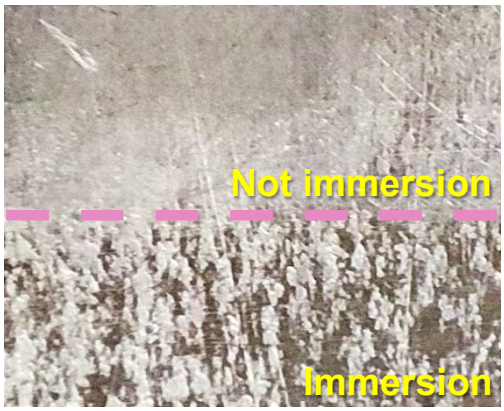

Fig. S6. The digital photo of Mo sheet counter electrode after constant potential electro-deoxidation at -0.2 V (vs. Pt) for 8 h.

After electro-deoxidation at -0.2 V (vs. Pt) for 8 h, the digital photo of Mo electrode was exhibited in Fig. S6. With the molten salt surface as the boundary, the Mo sheet shows different surface morphologies. The surface of Mo sheet immersed in the molten salt is relatively rough, and the surface which is not immersed in the molten salt is relatively smooth.

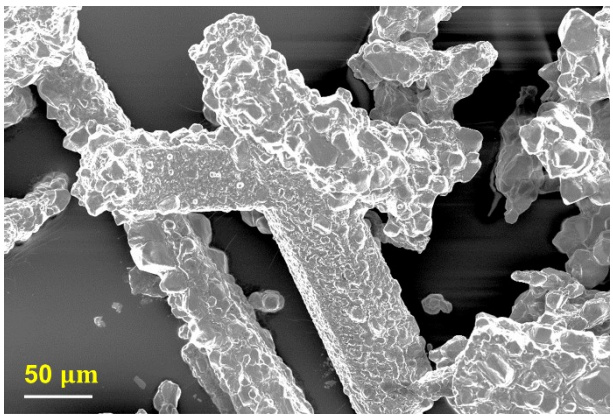

Fig. S7. SEM image of the product obtained at -0.05 V (vs. Pt).

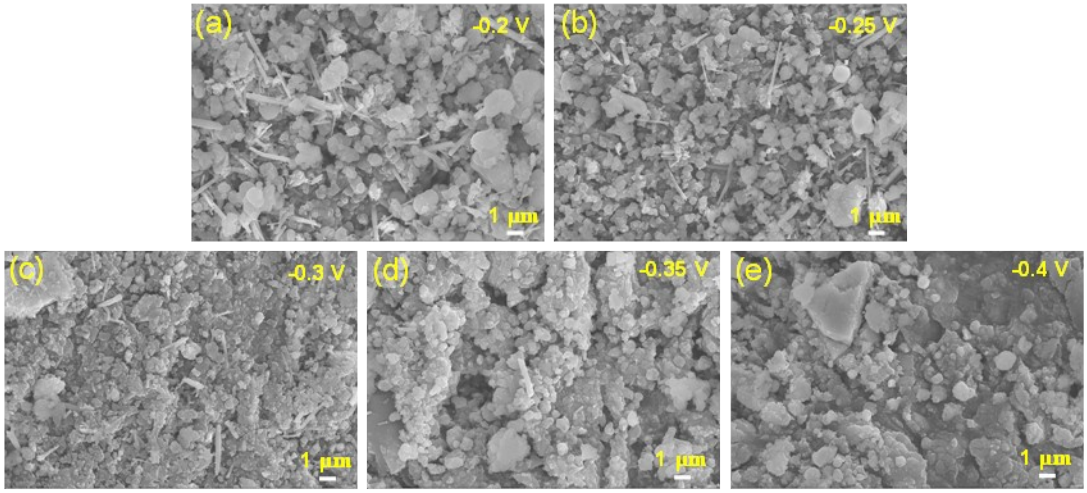

Fig. S8. Low-magnification SEM images of the products at different potentials.